

Submitted to ApJ Letter

The optical counterpart of a Ultraluminous X-Ray Object in M81

Ji-Feng Liu, Joel N. Bregman and Patrick Seitzer

Astronomy Department, University of Michigan, MI 48109

ABSTRACT

Ultraluminous X-Ray Objects are off-nucleus point sources with $L_X = 10^{39}$ - 10^{41} erg/s and are among the most poorly understood X-ray sources. To help understand their nature, we are trying to identify their optical counterparts by combining images from the Hubble Space Telescope and the Chandra Observatory. Here we report an optical counterpart for ULX NGC 3031 X-11, which has average X-ray luminosity of $\sim 2 \times 10^{39}$ erg/s and has varied by a factor of 40% over the last 20 years. We find a unique optical counterpart with the magnitude and color of an O8V star and we identify this as the secondary in a binary system. The primary is believed to be a black hole of approximately $18 M_\odot$, based on analyses of ACIS and ASCA spectra. This binary system probably is powered by mass transfer from the O8V star onto the black hole, with the Roche Lobe equal to the stellar radius. This model predicts an orbital period of ~ 1.8 days, which can be tested by future observations.

Subject headings: Galaxy: individual(M81) — X-rays: binaries

1. INTRODUCTION

X-ray emission from the nuclei of AGN and quasars, powered by accretion onto nuclear supermassive black holes, are usually $> 10^{41}$ erg/s, while for the stellar binary systems in the Milky Way, the luminosities are typically 10^{33} - 10^{38} erg/s. X-ray objects with luminosities of 10^{39} - 10^{41} erg/s have been observed in some external galaxies as off-nucleus point sources (Fabbiano 1989; Marston et al. 1995; Zezas et al. 2002). These objects have several names, the most popular designation being “Ultraluminous X-ray Objects”, or ULXs.

One suggestion for the nature of these ULXs is that they are binary systems with 10^3 - $10^4 M_\odot$ black holes as primaries (Colbert and Mushotzky 1999). This suggestion is

consistent with the X-ray spectra analyses of some ULXs (Makishima et al. 2000). However, the formation of such massive black holes is not predicted by stellar evolution theory and it may be impossible to form such objects even in dense star clusters. Alternatively, these sources may be stellar mass black holes or neutron stars whose emission is beamed, thereby representing micro-quasars (King et al. 2001). If the emission is beamed, the intrinsic luminosities become sub-Eddington, and there are known examples of beamed Galactic X-ray sources. It is also possible that the luminosities are truly super-Eddington, for example, obtainable from accretion disks with radiation-driven inhomogeneities (Begelman, 2002).

An essential step in uncovering the nature of the ULXs is to identify them at other wavelengths, such as optical. Associations of ULXs to emission-line nebulae based on ROSAT positions have already been done for a number of ULXs (e.g., Pakull & Mirioni, 2002). However, identifications down to single point sources were impossible given the large positional errors of EINSTEIN and ROSAT observations, with the smallest error circles had radii of $\sim 5''$ (for ROSAT HRI). With the advent of Chandra X-ray satellite, this task becomes possible owing to the sub-arcsecond spatial resolution of Chandra observations. For example, by comparing Chandra ACIS-S and HST/WFPC2 observations of the "Antennae" starburst galaxies, Zezas et al. (2002) found that 10 out of 14 ULXs are associated with stellar clusters, with offsets between the X-ray sources and the clusters less than $2''$. Wu et al. (2002) found that the ULX in edge-on spiral galaxy NGC4565 is associated with a stellar cluster on the outskirt of the bulge. Goad et al. (2002) found that within the $0''.6$ positional error circle of the ULX in NGC5204, there are three blue objects which they argue are very young stellar clusters.

As part of our search for optical counterparts of ULXs in nearby galaxies (Liu et al. 2001), we report the results for a ULX in NGC 3031, NGC 3031 X-11 as designated in Roberts & Warwick (2000). This ULX has been observed more than 20 times by EINSTEIN, ROSAT and Chandra X-ray satellites. Over the 20 year baseline, its X-ray luminosity varied by more than 40%, with an average of $\sim 2 \times 10^{39}$ erg/s. Matonick & Fesen (1997) found that this ULX is coincident with their SNR No. 22 and a discrete radio source in a VLA 20cm map, and suggested that it may be a SNR, despite its long term variability and high luminosity. In §2, we present the observations utilized, the data analysis procedures, and the results. We discuss the implications of its optical identification as an O8V star in §3. For the distance to M81, we use 3.63 Mpc ($\mu = 27.8 \pm 0.2$, Freedman et al. 1994). At such a distance, 1 pixel in the Planetary Camera chip, i.e., $0''.05$, corresponds to a physical scale of 0.9 parsecs.

2. OBSERVATIONS AND DATA ANALYSIS

NGC 3031 X-11 was observed by HST/WFPC2 in June, 2001 for our program. Three filters, F450W(B), F555W(V), and F814W(I) were used; for each filter, four 500-second exposures were made. We used HSTphot (Dolphin 2000) to perform PSF fitting photometry. To transform between WFPC2 image positions (X,Y) and celestial coordinates (RA,DEC), we used IRAF tasks `metric/invmetric`, which correct the geometric distortion introduced by the camera optics. The final relative positions are accurate to better than $0''.005$ for targets contained on one chip, and $0''.1$ for targets on different chips. The absolute accuracy of the positions obtained from WFPC2 images is typically $0''.5$ R.M.S. in each coordinate (HST data handbook).

A 50 kilosecond Chandra ACIS observation of NGC 3031 (ObsID 735, observed date: 2000-05-07) was retrieved from the Chandra archive. CIAO 2.2.1, CALDB 2.12 and `xspec` 11.2.0 were used to analyze the ACIS data. Pixel randomization of event positions was removed to recover the original positions. `Wavdetect` was run to detect discrete sources on ACIS-S chips. The accuracy of absolute positions for these sources has a typical R.M.S of $0''.6$ (Aldcroft et al. 2000).

Two bright X-ray sources fall into the WFPC2 field of view, i.e., the ULX on PC1 and SN 1993J on WF4, with a separation of $\sim 2'$. Using the relative position of these two sources, we can register the ULX onto the Planetary Chip very accurately. We list in Table 1 the ACIS and WFPC2 positions of SN 1993J, the ACIS position for the ULX, and its derived WFPC2 position. The centroiding error for ACIS-S3 positions computed by `Wavdetect` as quoted in Table 1 is negligible. The relative positional error comes mainly from the ACIS plate scale variation¹, which produces an error of $0''.1$ for a $2'$ separation, and the WFPC2 interchip error of $0''.1$. The rotation R.M.S. for both WFPC2 and ACIS-S chips are $\sim 0''.01$, and the resulted positional error is about $0''.02$. The final positional error is $\sim 0''.15$, i.e., about 3 Planetary Chip pixels. Within this error circle, there is only one object, which is indicated by a cross in Figure 1.

A cluster of typical size 2–3 parsecs, or a supernova remnant, can be readily resolved in the PC image. Careful examination shows that this unique counterpart of NGC 3031 X-11 is not extended, but a point source, with standard magnitudes $B = 23.87 \pm 0.04$, $V = 23.89 \pm 0.03$, and $I = 23.76 \pm 0.07$ as obtained with HSTphot. The counterpart is located on a dusty spiral arm and in a region of high stellar density, as can be seen in Figure 1. The Galactic extinction toward NGC 3031 are $A_B = 0.35$, $A_V = 0.27$, and $A_I = 0.16$,

¹see http://cxc.harvard.edu/cal/Hrma/hrma/optaxis/platescale/geom_public.html

with a HI column density² of $4.1 \times 10^{20} \text{ cm}^{-2}$ (Schlegel et al. 1998). When this extinction is removed, the counterpart has $M_B = -4.28$, $M_V = -4.18$, $M_I = -4.20$, $(B-V)_0 = -0.10$, and $(V-I)_0 = 0.02$. While its absolute magnitude is consistent with a O9V star ($19 M_\odot$, $7.8 R_\odot$; Schmidt-Kaler 1982), its color is much redder, which may indicate intrinsic extinction by its dusty environments. If we assume an intrinsic $E(B-V) = 0.22$ and a Galactic-like $R_V = 3.1$, the counterpart will have $M_V = -4.9$ and $B-V = -0.32$, matching the color and absolute magnitude of an O8V star ($23 M_\odot$, $8.5 R_\odot$), though the I band is dimmer by 0.1 magnitude. We note that the total color excess $E(B-V) = 0.3$ is consistent with the absorbing column density $2.1 \times 10^{21} \text{ cm}^{-2}$ derived from X-ray spectra according to a Galactic empirical relation $N_H = 5.8 \times 10^{21} * E(B-V)$ (Bohlin et al. 1979). This star is not a supergiant, since a supergiant is much redder and much brighter, for example, a B2I supergiant has $B - V = -0.17$ and $M_V = -6.4$.

3. DISCUSSION

The above determination of the mass and radius of the optical counterpart is based upon comparison with Galactic stars whose properties are known. Alternatively, one can try to obtain these quantities theoretically by comparing its observational properties to isochrones ($Z=0.020$) from the Geneva stellar models (Lejeune et al. 2001), such as in Figure 2, where we also show other bright stars in the field. The ages of the bright field stars are from about 10^6 to 10^8 years, with the anticipated implication that star formation in the spiral arm is not co-eval. The location of the counterpart in the color-magnitude diagram is consistent with it being a star younger than $10^{6.5}$ years. If it has spent $10^{6.5}$ years on the main sequence, its absolute magnitude corresponds to that of a star with a mass of $27 M_\odot$ and a radius of $10.0 R_\odot$. A limiting case is that it is a star that has just reached the main sequence, which makes it hotter and more massive, with a mass of $41 M_\odot$ and a radius of $8.7 R_\odot$. The stellar metalicity may differ from solar, which will lead to small changes in the inferred mass and radius, so we consider two extreme cases of low and high metalicity. For a star of metalicity $Z=0.004$, the age would be less than $10^{6.7}$ years from its location on the Main Sequence, and its mass ranges from 50 to $28 M_\odot$ with a radius between 8.3 to $10.3 R_\odot$ with increasing age. For a star of metalicity $Z=0.040$, it would be younger than $10^{6.4}$ years, its mass lies between 36 and $26 M_\odot$ with a radius between 8.8 and $9.8 R_\odot$. Taking into account the range of possibilities, the inferred mass is between 26 and $50 M_\odot$, and the radius is between 8.3 and $10.3 R_\odot$. This result can be compared to the mass and radius inferred from its spectral type, i.e., $23 M_\odot$ and $8.5 R_\odot$ for an O8V star. We conclude that the radius is about 9.3 ± 1.0

²<http://heasarc.gsfc.nasa.gov/cgi-bin/Tools/w3nh/w3nh.pl>

R_{\odot} , while the mass is somewhat uncertain, ranging from 23 to $50 M_{\odot}$. The lower end of this mass range is preferred because it is unlikely that the star has just reached the main sequence since its binary companion has already evolved into a compact object. This optical counterpart is presumably a secondary in a binary system, and is contributing material onto an accreting compact primary.

Swartz et al. (2002) analyzed the radial profile of this ULX in their Chandra ACIS-S3 observation, and found it consistent with a point source; it is consistent with a point source in our WFPC2 observations. They also analyzed the spectrum and found, after deconvolving the effects of pileup, the spectrum is best described by a model for an absorbed blackbody disk. The best-fit absorbing column density is $N_{20} = 21.7 \pm 1.0$ in units of 10^{20} cm^{-2} ; the best-fit innermost disk temperature is $T_{in} = 1.03 \pm 0.11 \text{ Kev}$, the corresponding radius is $R_{in} = 161 \pm 16 \text{ km}$, which correspond to an $18 M_{\odot}$ non-rotating black hole. From an analysis of ASCA spectra, Mizuno (2000) found the following parameters, $N_{20} = 21 \pm 3$, $T_{in} = 1.48 \pm 0.08 \text{ Kev}$, $R_{in} = 83 \pm 8 \text{ km}$, which he argued correspond to a Kerr black hole with similar mass. In Figure 3, we compared the fluxes of the counterpart in B, V, and I bands with the predictions of the absorbed disk blackbody model derived from Chandra ACIS and ASCA spectra, and found that the observed optical fluxes are at least 10-30 times brighter than the disk itself, indicating that most of the optical flux is from the X-ray inactive secondary O8V star. Furthermore, the optical disk has a color of $B-V \approx 0.1$, which is significantly flatter (redder) than the color of the counterpart. These two pieces of evidence lead us to conclude that the optical light is from a star rather than from an accretion disk.

The nature of the X-ray variability, the X-ray spectral properties, and the optical colors indicate that NGC 3031 X-11 is not a supernova remnant (Matonick & Fesen 1997) but is a high mass X-ray binary (HMXB) system, consisting of an $M_1 = 18 M_{\odot}$ black hole and an $M_2 = 23 M_{\odot}$ O8V companion. HMXB systems in our Galaxy with black hole masses above about $10 M_{\odot}$ have $L_X < 10^{39} \text{ erg/s}$, with very few exceptions. An example is Cygnus X-1, which has a BH of $15 M_{\odot}$ and a companion of O9.7Iab supergiant, with $L_X < 10^{38} \text{ erg/s}$ (Tanaka & Lewin, 1995). These modest luminosities can be understood given the low accretion efficiency of stellar wind from the companion supergiants. For this ULX system, since the companion is a main sequence star, its stellar wind is not as strong as supergiants, and it may be accreting gas via Roche Lobe Overflow.

This scenario can be tested by future observations. Black hole masses derived from spectral analyses are best fits to simple models, so changes to the models, especially for the inner region, may lead to different masses. In addition, there is the concern that stellar evolutionary models do not predict $18 M_{\odot}$ black holes. For example, models for $60 M_{\odot}$ main sequence stars at the point of core collapse (Vanbeveren et al. 1998, and references therein)

predict a mass of $\sim 11M_{\odot}$. These uncertainties in the mass determination can be avoided by obtaining a direct measure of black hole mass (function) through measurements of an orbital period and the associated orbital velocities.

We can predict the period of the binary based on the mass of the secondary and the requirement that it is filling its Roche lobe. If the counterpart has the radius and mass of an O8V star, i.e., a radius of $\sim 8.5R_{\odot}$ and a mass of $23M_{\odot}$, we infer that the separation between the primary and secondary is $a = (0.6q^{2/3} + \ln(1 + q^{1/3}))q^{-2/3}/0.49R_{cr} \approx 21R_{\odot}$ for their mass ratio $q = M_2/M_1 \approx 1.3$ (Eggleton 1983). This in turn implies an orbital period of $P_{orb} \approx 1.8$ days according to Kepler's 3rd law. For the mass range of $23\text{-}50 M_{\odot}$ and the radius range of $9.3 \pm 1.0 R_{\odot}$, the expected orbital period ranges from 1.1 days to 2.1 days. Although challenging, the measurement of the period would greatly illuminate the nature of this, and presumably other ULX systems.

King et al. (2001) raised the possibility that ULXs could be HMXB systems during their short thermal timescale mass transfer via Roche Lobe overflow, and our identification of ULX NGC 3031 X-11 with an O8V star supports this idea. Such high mass systems have very short ages, consistent with the general findings that ULXs tend to occur in star forming regions (e.g., Zezas et al. 2002). However, ULXs also occur in some elliptical galaxies, e.g., NGC 1399 (Angelini et al. 2001), and those may be intrinsically different from what we discuss here.

We are grateful for the service of Chandra Data Archive. We would like to thank Jimmy Irwin, Renato Dupke, Eric Miller, Rick Rothschild, and Steven Murray for helpful discussions. We gratefully acknowledge support for this work from NASA under grants HST-GO-09073.

REFERENCES

- Aldcroft, T.L., Karovska, M., Cresitello-Dittmar, M.L., Cameron, R.A., and Markevitch, M.L., 2000, Proc. SPIE, 4012, 650
- Angelini, L., Loewenstein, M., and Mushotzky, R.F., 2001, ApJ, 557, L35
- Begelman, M.C., 2002, ApJ, 568, L97
- Bohlin, R., avage, B.D., and Drake, J.F., 1978, ApJ, 224, 132
- Colbert, E.J.M. and Mushotzky, R.F., 1999, ApJ, 519, 89

- Dolphin, A.E., 2000, PASP, 112, 1383
- Eggleton, P.P., 1983, ApJ, 268, 368
- Fabbiano, G. 1989, ARA&A, 27, 87
- Freedman, W.L., Hughes, S. M., Madore, B. F. et al., 1994, ApJ, 427, 628
- Goad, M.R., Roberts, T.P., Knigge, C., and Lira, P. 2002, astro-ph/0207428
- King, A.R., Davies, M.B., Ward, M.J., Fabbiano, G., and Elvis, M. 2001, ApJ, 552, L109
- Lejeune, T. and Schaerer, D., 2001, A&A 366, 538
- Liu, J., Bregman, J.N., and Seitzer, P., 2001, AAS, 199, 0503
- Marston, A.P., Elmegreen, D., and Elmegreen, B. 1995, ApJ, 438, 663
- Makishima, K., Kubota, A., Muzuno, T., Ohnishi, T., Tashiro, M., et al. 2000, ApJ, 535, 632
- Mizuno, T., 2000, Ph.D. Thesis, Univ. Tokyo
- Matonick, D.M. and Fesen, R.A. 1997, ApJSS, 112, 49
- Pakull, M.W. and Mirioni, L., 2002, astro-ph/0202488
- Roberts, T.P. and Warwick, R.S., 2000, MNRAS, 315, 98
- Schmidt-Kaler, Th., 1982, *Landolt-Bornstein: Numerical Data and Functional Relationships in Science and Technology*, eds. Schaifers, K. and Voigt, H.H., VI/2b, P.15-31
- Schlegel, D.J., Finkbeiner, D.P., and Davis, M., 1998, ApJ, 500, 525
- Swartz, D.A., Ghosh, K.K., McCollough, M.L., Pannuti, T.G., Tennant, A.F., and Wu, K., 2002, astro-ph/0206160
- Tanaka, Y. and Lewin, W.H.G. 1995, in *X-ray Binaries*, eds. Lewin, W.H.G, van Paradijs, J., and van den Heuvel, E.P.J. P.265
- Vanbeveren, D., de Loore, C., and van Rensbergen 1998, A&ARev, 9, 63
- Wu, H., Xue, S.J., Xia, X.Y., Deng, Z.G., and Mao, S.D. 2002, astro-ph/0204359
- Zezas, A., Fabbiano, G., Rots, A.H., and Murray, S.S. 2002, astro-ph/0203175

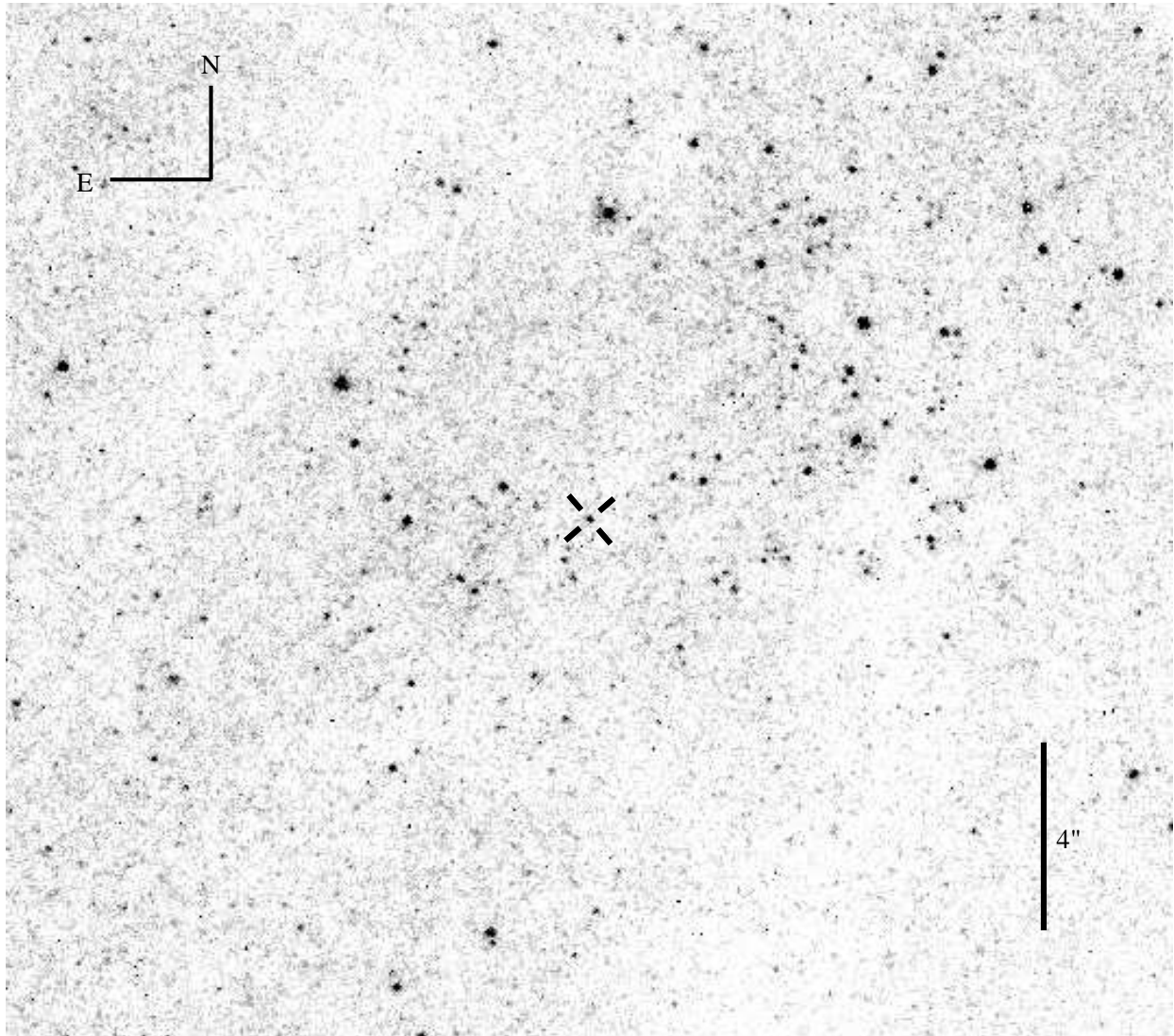


Fig. 1.— The optical counterpart of NGC 3031 X-11 and its environments. The counterpart, indicated by a cross, is a point source with standard magnitudes $B = 23.87 \pm 0.04$, $V = 23.89 \pm 0.03$, and $I = 23.76 \pm 0.07$. When the Galactic and intrinsic extinction is removed, its absolute magnitude and colors correspond to those of an O8V star. The size of the image is about $22'' \times 22''$ and the distance between the inner edges of two diagonal line segments of the cross is twice the diameter of the positional error circle of the counterpart.

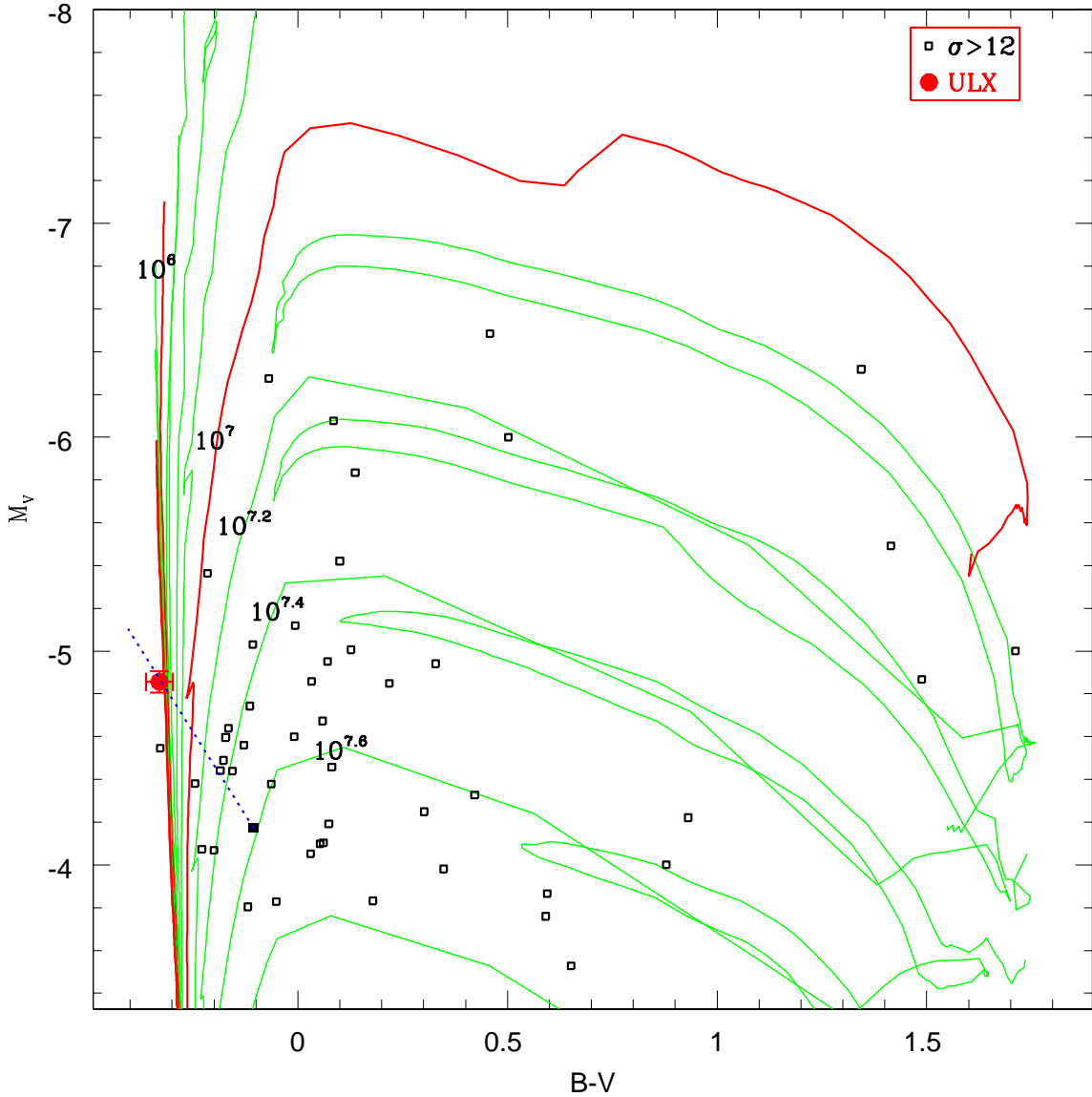


Fig. 2.— Color magnitude diagram for the ULX and nearby bright stars with signal-to-noise ratio $\sigma > 12$. Galactic extinction is removed from all the stars and the counterpart also is corrected for intrinsic extinction, as inferred from its X-ray absorption. The stellar isochrones are taken from Lejeune et al. (2002) for $Z=0.020$ and the dashed line indicates the de-reddening vector for HI absorption assuming $R_V = 3.1$.

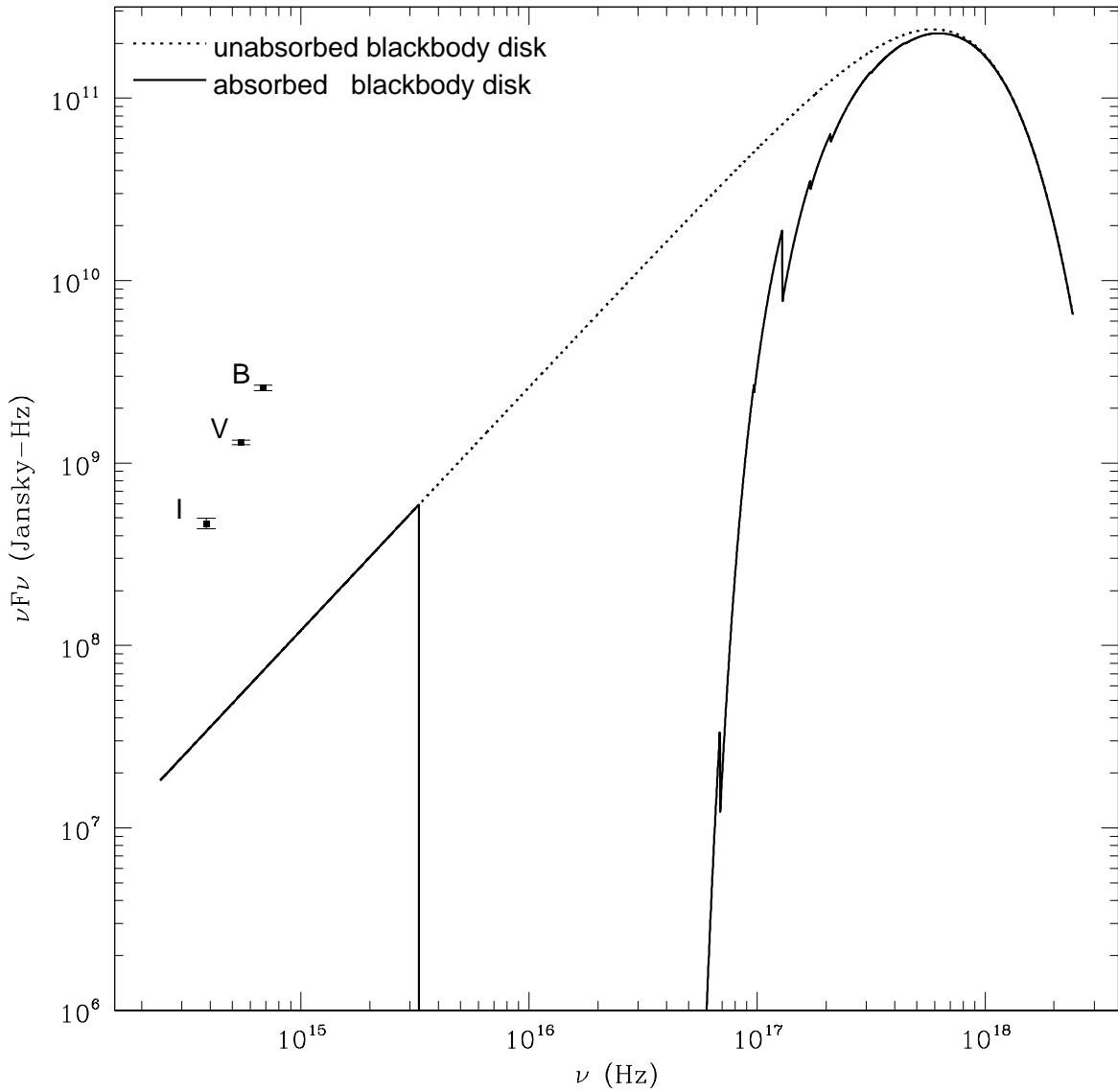


Fig. 3.— Spectral energy distribution of NGC 3031 X-11. The X-ray spectra from ACIS can be fitted by an absorbed disk blackbody model, which we extend down to optical to compare with the B, V, and I photometry of the counterpart. Both the model and the BVI magnitudes are dereddened. The BVI fluxes of the counterpart are 30-10 times larger than the disk itself.

Table 1. The optical counterpart for ULX NGC 3031 X-11

Object	ACIS-S3				WFPC2				
	RA	DEC	RA_ERR (arcsec)	DEC_ERR (arcsec)	Chip	X (pix)	Y (pix)	RA	DEC
SN 1993J	9:55:24.79	69:01:13.44	0.03	0.01	4	480.72	240.89	9:55:25.11	69:01:14.87
NGC 3031 X-11	9:55:32.95	69:00:33.36	0.03	0.01	1	437.57	408.32	9:55:33.27	69:00:34.79